Calculations of the threshold force and threshold power to move adsorbed nanoparticles

Dhavide A. Aruliah
Faculty of Science, University of Ontario Institute of Technology, Oshawa, Ontario, L1H 7K4, Canada

Martin H. Müser*
Department of Applied Mathematics, University of Western Ontario, London, Ontario N6A 5B7, Canada

Udo D. Schwarz
Department of Mechanical Engineering, Yale University, P.O. Box 208284, New Haven, CT 06520-8284, USA

(Dated: October 15, 2004)

We propose and analyze a simple model for the calculation of the power P^* necessary to depin an essentially rigid cluster or nanoparticle on a surface with a scanning force microscope tip in tapping mode. The model contains the coupling between the particle's lateral and normal motion. We show that there are two important limiting regimes: (i) If momentum transfer occurs gradually between tip and particle, P^* depends mainly on the viscous-type drag between particle and surface. (ii) If momentum transfer occurs instantaneously once per oscillation, P^* is dominated by the minimum energy barrier necessary to move the cluster by one lattice constant. In the quasi-static driving mode (i), a critical impact angle $\alpha_{\rm t}^*$ is identified below which depinning cannot be achieved due to lateral-normal coupling.

I. INTRODUCTION

In recent experiments, a scanning force microscope (SFM) tip is used to probe various islands or clusters ("nanoparticles") of antimony atoms adsorbed on either graphite or on MoS_2 substrates.[1] These islands or particles with a linear dimension in the order of 100 to 300 nm self organized after thermal evaporation of solid antimony. The SFM tip impacts such self-organized nanoparticles in tapping mode while the power loss P of the SFM tip is recorded for each individual cluster.[1] The experiments show that an island becomes mobile only when P exceeds a threshold value P^*; for $P < P^*$, the nanoparticle remains pinned at their initial positions. Analysis indicates that the antimony clusters appear generally undamaged during the experiments. The full interpretation of these experiments remains an open question; specifically, it is not known whether or not P^* can be related to the static friction force $F_{\rm s}$, some kind of activation energy ΔE or to phononic-type damping. In general, it would be desirable to understand what energy is required to translate adsorbed particles on surfaces, as there is an increasing experimental body of work that is concerned with the mechanical manipulation of adsorbed nanoparticles (see, e.g., Refs. 2–7).

Large-scale computer simulations are certainly helpful to more fully address the detailed atomistic dynamics of the experiments sketched above. In particular, a simulation can include many important aspects (such as long-range elastic deformations of the SFM tip and the sample) more readily than a primarily analytical approach can. However, as a first step, we attempt to discover the relation between P^* and various parameters ($F_{\rm s}$, phononic drag, tip frequency, etc.) by studying a highly idealized model that includes some of the experiments' key features. The main approximation in our treatment is that the cluster is treated as a rigid body, i.e., we assume that elastic deformation occurs instantaneously and that its effects can be 'absorbed' into effective interactions. However, we specifically want to account for the coupling between lateral and normal motion of the rigid body as it moves on the substrate, i.e., the harder the island is pressed by the tip into the substrate the higher the expected lateral force between island and substrate. Although we would prefer a generic case study, our model requires certain *ad hoc* assumptions about the pair-wise interactions between the bodies involved: the antimony cluster, the graphite substrate, and the SFM tip in tapping mode. However, once the model is defined, it is possible to investigate how the adsorbed islands moves under the influence of a periodically oscillating SFM tip and which parameters affect the motion and hence energy dissipated in the experiment.

Several theoretical arguments and computer simulations suggest that each atom in a dry contact of two chemically passivated solids has only one mechanical stable position once the contacting solids' relative center of mass and orientation is known.[8] Thus, we will assume that no bond breaking occurs during the experiments and that the two solids can be treated as effectively rigid objects. Under these circumstances, coupling to internal lattice vibrations (or to other dynamical modes that quickly find local thermal equilibrium) primarily leads to a drag force linear in the instantaneous, relative sliding velocity. With these assumptions in mind as well as the substrate's periodicity, it is possible to define a rather generic model for the interaction between nanoparticle and substrate. Modeling the force between an SFM tip in tapping mode and the adsorbed island unfortunately

leaves us with many possibilities. For instance, it is not obvious whether momentum is transferred gradually or abruptly from the tip to the sample. Therefore, we will consider two limiting cases; one in which momentum transfer occurs instantaneously once per tip oscillation, and one in which the momentum is transfered gradually with the frequency of the tip.

In the next section, we will introduce our model in detail. In Sect. III, we will discuss analytically available solutions for the dynamics, in particular the quasi-static motion of the cluster and a quasi-harmonic approximation to the problem. Sect. IV contains a comparison between numerical solutions of the equations of motion and the various analytical solutions. We will conclude in Sect. V.

II. MODEL

We first consider a straightforward model for the conservative and the non-conservative forces between the island and the substrate. The free model parameters are not yet specified. However, they will be related to experimentally available data such as static friction force F_{s} and interfacial stiffness in Section III. We will also discuss the coupling between tip and substrate.

A. Particle-substrate interaction: Cobblestone model

The cobblestone model in its original form considers the interaction between two essentially non-deformable but rough surfaces.[9] The model therefore implies the argument going back to Euler that one solid body has to climb up an effective slope in the initial sliding process. This in turn implies proportionality of lateral and normal force given a relative lateral position of the two solid bodies in contact. Here, we intend to discuss an interaction potential amenable to simple analytical calculation that has the cobblestone property.

For simplicity, we consider a two-dimensional model that includes coupling between lateral and normal motion. Let x and z denote the horizontal and vertical coordinates respectively; then z is the normal distance between the adsorbed particle and the substrate. Following Steele's construction of atomic substrate potentials,[10] at a fixed height z, the interaction potential $V_{\mathrm{sub}}(x,z)$ between an essentially rigid nanoparticle and a periodic substrate is periodic in the lateral direction x with period $2\pi a$ (also called the lattice constant of the substrate). Thus, as a first approximation,

$$V_{\mathrm{sub}}(x,z) = \tilde{V}_0(z) + \tilde{V}_1(z)\cos(x/a) + \tilde{V}_2(z)\cos(2x/a) + \cdots, \quad (1)$$

where the expansion coefficients $\tilde{V}_n(z)$ depend on z alone. If r is the distance between two atoms, the repulsive portion of inter-atomic potentials is often of the form $\exp(-r/\sigma)$ for some suitable length constant σ thus, we assume a similar behavior in the lateral dependence of the coefficients in Eq. (1), namely

$$\tilde{V}_n(z) = V_n e^{-z/\sigma_n}, \quad (2)$$

for some coefficients V_n and σ_n. We assume further that the coefficients σ_n depend weakly on n, i.e., $\sigma_n = \sigma =$ constant for all n. (Varying σ_n violates the linear lateral force versus normal-load relationship, which can be seen by taking the first partial derivative of $V(x,z)$ with respect to x and with respect z.)

Since our arguments extend to three dimensions, we use A to refer to the measure or generalized area of the region of contact. In our two-dimensional model, A is actually the length of a one-dimensional line of contact measured in units of σ. Consider the dependence of the coefficients V_n in Eq. (2) on A. Now, since $\tilde{V}_0(z)$ in Eq. (1) is independent of the corrugation of the surface, the coefficient V_0 must be linear in A irrespective of the surface's periodic symmetry. Hence, for some constant of proportionality v_0, $V_0 = Av_0(z)$. Higher-order terms V_n in the substrate potential are linear in A only if the two surfaces manage to lock together perfectly, i.e., only if they are commensurate. In general, V_1 is expected to show non-trivial dependence on A, e.g., $\langle |V_1|^2 \rangle \propto A$ if one of the two surfaces is disordered.[11] In the following calculations, we will assume fixed values for A, V_0, and V_1. However, for the purpose of a general discussion, we have included which scaling of V_0 and V_1 with A one might expect.

Neglecting terms above $n = 1$ in Eq. (1), the substrate potential V_{sub} is given by

$$V_{\mathrm{sub}}(x,z) = e^{-z/\sigma}\left(V_0 + V_1\cos(x/a)\right). \quad (3)$$

From the argument in the preceding paragraph, $V_0 = v_0 A$, so we can write

$$V_{\mathrm{sub}}(x,z) = v_0 A e^{-z/\sigma}\left(1 - \frac{\mu a}{\sigma}\cos(x/a)\right), \quad (4)$$

where $\mu := -(\sigma V_1)/(aV_0)$ is a coefficient that depends on A in principle. To make Eq. (4) nondimensional, choose σ as the unit of length and v_0 as the unit of surface energy per unit of length or area. Thus, when we add a load F_{l} (either externally imposed or adhesive), the total dimensionless potential of the adsorbed particle is

$$V(x,z) = F_{\mathrm{l}} z + Ae^{-z}\left(1 - \mu a\cos(x/a)\right). \quad (5)$$

The inclusion of a constant (adhesive) load F_{l} in the potential V is simplistic but using a more realistic load leaves the main conclusions unaltered. Similar potentials have been used to model tribological systems,[12] in particular to study the coupling of normal and lateral motion. We show below that the present choice of V reproduces the linear relationship between friction force and external load (as manifested in Amontons's law[8]).

Furthermore, this potential implies that the interfacial stiffness varies linearly with $F_{\rm l}$ (which has indeed been observed experimentally[13]).

When the island moves at finite velocities, it is subject to normal and corrugation forces and its motion couples to lattice vibrations within the substrate or other quickly equilibrating internal degrees of freedom. This coupling is typically described by a simple Stokes damping mechanism plus thermal fluctuations.[8] Disregarding thermal fluctuations, whose effects can be mimicked by stochastic random forces, the equation of motion is

$$A\rho h \begin{pmatrix} \ddot{x} \\ \ddot{z} \end{pmatrix} + A \begin{pmatrix} \gamma_x & 0 \\ 0 & \gamma_z \end{pmatrix} \begin{pmatrix} \dot{x} \\ \dot{z} \end{pmatrix} + \begin{pmatrix} \partial V/\partial x \\ \partial V/\partial z \end{pmatrix} = \begin{pmatrix} F_x(t) \\ F_z(t) \end{pmatrix}, \tag{6}$$

where γ_x and γ_z respectively denote the lateral and normal damping coefficients per unit area per unit velocity, h denotes the average height of the island, and ρ denotes the nanoparticle's mass density. Although the coefficients γ_x and γ_z almost certainly depend on the vertical distance between the island and the substrate, we disregard this dependence in our analytical calculations. While it is not too difficult to account for such effects in practical numerical calculations, we intend to keep the number of *ad hoc* parameters as small as possible. Moreover, it is conceivable that the external normal force is small compared to the adhesive load and that the variations of the damping coefficients during the experiment are negligibly small.

We choose ρh to be the unit of mass per unit area. Thus, $\rho h\sigma^2$ corresponds to the unit of mass and rewriting in terms of dimensionless units, Eq. (6) becomes

$$\begin{pmatrix} \ddot{x} \\ \ddot{z} \end{pmatrix} + \begin{pmatrix} \gamma_x & 0 \\ 0 & \gamma_z \end{pmatrix} \begin{pmatrix} \dot{x} \\ \dot{z} \end{pmatrix} + \frac{1}{A} \begin{pmatrix} \partial V/\partial x \\ \partial V/\partial z \end{pmatrix} = \frac{1}{A} \begin{pmatrix} F_x \\ F_z \end{pmatrix}. \tag{7}$$

The external force $\mathbf{F} = (F_x, F_z)^T$ in Eq. (7) represents the interaction between tip and island and is described below.

All our results will be free of units, because the three mechanical units have been defined through σ, v_0, and ρh. Without loss of generality, we assume the island's area of contact to be equal to unity as well.

B. Tip-particle coupling

Consider the system's geometry as shown in Fig. 1. To model the contact mechanism between the nanoparticle and the SFM tip, our main assumption is that the contact region is sufficiently small that the local geometry of the SFM tip is that of a flat wedge inclined at an angle $\alpha_{\rm t}$ from the horizontal. Thus, it is possible to treat the tip-particle interaction as a wedge-particle interaction, i.e.,

$$\mathbf{F} = \begin{pmatrix} F_x \\ F_z \end{pmatrix} := F(t) \begin{pmatrix} \sin\alpha_{\rm t} \\ -\cos\alpha_{\rm t} \end{pmatrix} \tag{8}$$

where $F(t)$ is the time-dependent amplitude of the external force applied. Using Eq. (8), we implicitly assume

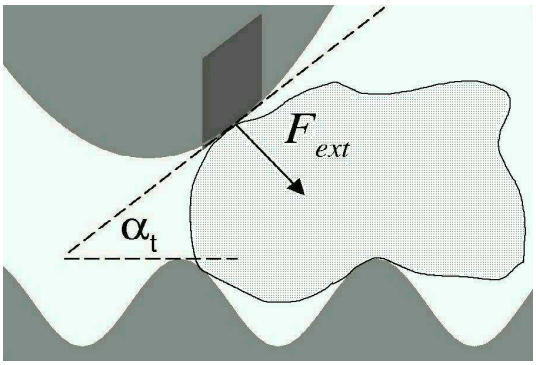

FIG. 1: Schematic of SFM tip-particle coupling. The SFM tip is locally approximated by a flat wedge. The angle of inclination $\alpha_{\rm t}$ decomposes the force $\mathbf{F}$ into normal and transversal components.

that the SFM tip in tapping mode moves mostly in the vertical direction and that small fluctuations of the island's position has little influence on the impact angle $\alpha_{\rm t}$. Furthermore, we assume that the area of contact on the island can also be approximated by a wedge near the point of impact and that its local slope is the same as that of the tip. Knowing the relationship Eq. (8) between the normal and lateral external force components greatly simplifies all following calculations.

It is not generally possible to specify the external driving force F that the tip exerts on the sample (e.g., there may be a feedback mechanism between the sample's motion to the tip's motion). However, once the system reaches its steady state under oscillatory driving, $F(t)$ must have the same time period as the SFM tip's vertical motion while the nanoparticle remains pinned. Thus, as long as the island remains stable, $F(t)$ can be written as a Fourier sum

$$F(t) = \sum_n F_n e^{in\omega_{\rm t} t}, \tag{9}$$

where $\omega_{\rm t}$ is the tip's tapping frequency and F_n are Fourier coefficients.

In our treatments that follow, two limits are analyzed regardless of whether they use a the full island-substrate potential or small-amplitude approximation. In the first limit, only small frequencies $n\omega_{\rm t}$ are considered relevant, i.e. F_0 and F_1 dominate the time-dependent contribution in Eq. (9). For the second limit, we assume the momentum transfer occurs in time with the SFM tip's period, in which case F_n does not depend on the Fourier index n. The actual behavior in experiments lies somewhere between these two extremes.

III. THEORY

A. Equilibrium Analysis

Consider the system described by Eq. (7) under adiabatic or quasi-static driving. It is in an equilibrium state $(x_{\rm eq}, z_{\rm eq})$ when the gradient of the potential V in Eq. (5) exactly balances the external driving force $\mathbf{F}$ in Eq. (8), i.e.,

$$\left.\frac{\partial V}{\partial x}\right|_{(x_{\rm eq},z_{\rm eq})} = F_x, \tag{10a}$$

$$\left.\frac{\partial V}{\partial z}\right|_{(x_{\rm eq},z_{\rm eq})} = F_z. \tag{10b}$$

Before deriving the general solution of the system Eq. (10), it is instructive to consider a specialized system to gain insight into the interpretations of the model's parameters.

1. Equilibrium analysis of system under lateral force

In many cases, friction forces are measured under a constant normal load rather than under a time-dependent load, which we effectively obtain if $\alpha_{\rm t} \neq \pi/2$ in Eq. (8). We will therefore discuss time-dependent lateral driving first by examining the mechanically stable position as a function of external lateral force at constant (adhesive) load $F_{\rm l}$. For this special case and provided μa is sufficiently small, we will show that the maximum lateral force $F_{\rm s}$ that the substrate can exert on the cluster satisfies $F_{\rm s} = \mu F_{\rm l}$, so that we may interpret μ as a friction coefficient. Moreover, the energy difference between the point of smallest and largest potential energy can be approximated by $\Delta E_{\rm min} \approx 2aF_{\rm s}$ for small values of μa. The remainder of this section will be concerned with the calculations leading to these results.

Assume for the moment that the applied force is strictly lateral, i.e., that $\alpha_{\rm t} = \pi/2$ in Eq. (8). As a result, the normal equilibrium coordinate $z_{\rm eq}$ is determined by requiring $\partial V(x_{\rm eq}, z_{\rm eq})/\partial z = 0$ in Eq. (10b). Under this assumption, $z_{\rm eq}$ is a unique function of $x_{\rm eq}$, namely

$$z_{\rm eq}(x_{\rm eq}) = -\ln\left(\frac{F_{\rm l}/A}{1-\mu a\cos(x_{\rm eq}/a)}\right) \tag{11a}$$

$$\approx -\ln(F_{\rm l}/A) - \mu a\cos(x_{\rm eq}/a), \tag{11b}$$

where the approximation Eq. (11b) is valid when μa is sufficiently small. From Eq. (11a), the maximal gradient of $z_{\rm eq}$ with respect to $x_{\rm eq}$ is $\mu/\sqrt{1-\mu^2a^2}$. Thus, Eq. (11) shows that μ is the steepest gradient up which the island climbs while moving on the substrate under lateral quasi-static driving in the limit as $\mu a \to 0$.

To maintain quasi-static driving, the lateral component of the external force must balance the force induced by the substrate potential. This condition implies $F_x = \partial V(x_{\rm eq}, z_{\rm eq}(x_{\rm eq}))/\partial x$, so

$$F_x = A\mu e^{-z_{\rm eq}(x_{\rm eq})}\sin(x_{\rm eq}/a). \tag{12}$$

The magnitude of F_x in Eq. (12) is extremal when $\tan(x_{\rm eq}/2a) = \sqrt{(1+\mu a)/(1-\mu a)}$. This equality has two consequences: (i) The x position where F_x is maximal is (slightly) shifted with respect to the value $a\pi/2$, which one would expect from a simple sinusoidal tip-substrate potential $-V\cos(x/a)$ reflecting lateral-normal coupling only to lowest order. (ii) The maximum lateral or static friction force is

$$F_{\rm s} := \text{maximum lateral or static friction force}$$

$$= \frac{\mu F_{\rm l}}{\sqrt{1-\mu^2a^2}} \tag{13a}$$

$$\approx \mu F_{\rm l} \tag{13b}$$

in the limit as $\mu a \to 0$. Notice that even when using a more realistic adhesive term in the potential V in Eq. (5) (e.g., a Morse potential), the interpretation of μ as a maximum slope of the island's spatial trajectory remains true even though a different maximum static friction force $F_{\rm s}$ results in Eq. (13).

Having derived $z_{\rm eq}(x_{\rm eq})$, the energy at the top of the barrier $E_{\rm max} = V(\pi a, z_{\rm eq}(\pi a))$ at fixed load $F_{\rm l}$ is $E_{\rm max} = F_{\rm l}\left[1+\ln\{A(1+\mu a)/F_{\rm l}\}\right]$. Since the ground state energy $E_{\rm min}$ is $E_{\rm min} = V(0, z_{\rm eq}(0)) = F_{\rm l}\left[1+\ln\{A(1-\mu a)/F_{\rm l}\}\right]$, we compute the optimum energy barrier $\Delta E_{\rm min}$ as

$$\Delta E_{\rm min} := E_{\rm max} - E_{\rm min}$$

$$= F_{\rm l}\ln\left(\frac{1+\mu a}{1-\mu a}\right) \tag{14a}$$

$$\approx 2aF_{\rm s} \tag{14b}$$

in the limit as $\mu a \to 0$. The energy barrier $\Delta E_{\rm min}$ is a lower bound on the amount of energy needed to displace an adsorbed nanoparticle at rest from one minimum to the next laterally adjacent minimum (starting from rest and under a constant normal load).

We wish to conclude this section with a discussion on the position $x^*_{\rm eq}$ where the particle would become unstable if the lateral external force was ramped up very slowly with time. The condition for this to happen is mentioned in the text following Eq. 12, i.e., for small lateral-normal coupling (μ is close to zero), it would occur at $x^*_{\rm eq} \approx a\pi/2$. This corresponds to a result found by Gnecco et al.[14], who studied the friction between an atomic force microscope tip and a substrate within the Tomlinson model, which does not include lateral normal coupling explicitly. They found the same depinning position in the limiting case where the driving spring is extremely compliant and moved very slowly. In this limit one can show that the (external) force from the spring on the particle is essentially constant in time[8], which corresponds to the situation discussed in our stability analysis. We may add that when moving quasi-statically, our object can be interpreted to be part of the tip. Conversely,

it is often believed that atomic force microscope tips are contaminated with material from the substrate which is slid against genuine substrate. This justifies the comparison between Gnecco et al.'s[14] and our study.

2. General equilibrium analysis

We will now be concerned with the analysis of the quasi-static dynamics of the cluster when it is driven by an oscillatory force with slowly-varying amplitude F under an arbitrary impact angle $\alpha_{\rm t}$. It will be shown that there is a critical value $\alpha_{\rm t}^*$ for the impact angle below which the cluster will remain pinned in the model, no matter how large F. For $\alpha > \alpha_{\rm t}^*$, there is a critical threshold F^* for the force amplitude above which the particle cannot remain pinned.

Including the effect of arbitrary impact angle, one would has to replace the load $F_{\rm l}$ in Eq. (11a) with $F_{\rm l}-F_z$, where $F_z = -F_0 \cos\alpha_{\rm t}$ represents the z-component of the force that the tip exerts on the island, thus,

$$z_{\rm eq} = -\ln\left(\frac{(F_{\rm l}-F_z)/A}{1-\mu a\cos(x/a)}\right). \tag{15}$$

Consequently, the lateral equilibrium position for a given external force must satisfy:

$$(F_{\rm l}-F_z)\frac{\mu\sin(x_{eq}/a)}{1-\mu a\cos(x_{eq}/a)} = F_x, \tag{16}$$

where $F_x = F_0\sin\alpha_{\rm t}$ is the x component of the tip force. (This equation follows from adding a potential energy term $-(F_x x + F_z z)$ to the potential energy of the island and requiring that the derivative of the total potential with respect to x must be zero.) This equation can be solved for (positive) $\cos(x_{eq}/a)$, resulting in

$$\cos(x_{eq}/a) = \frac{\tilde f^2 + \sqrt{\tilde\mu^2(1+\tilde f^2)-\tilde f^2}}{\tilde\mu(1+\tilde f^2)}, \tag{17}$$

where we have introduced the reduced lateral force $\tilde f = F_x/\{a(F_{\rm l}-F_z)\}$ and the reduced atomic friction coefficient $\tilde\mu = \mu a$. Substituting Eq. (17) into Eq. (15) then yields the rigid body's mechanically stable z position as a function of load $F_{\rm l}$ and force amplitude F_0.

If the external force is varied very slowly so that the tip is always at its mechanical equilibrium position at every instance of time, one can calculate the tips trajectory as a function of time and the threshold force F_0, at which the island is starting to become unstable. The instability occurs when Eq. (17) has no more (stable) solution upon increasing F_0, for instance, when the argument of the square root on the right-hand side of Eq. (17) becomes negative. Thus, we obtain the following threshold value $\tilde f^*$ for the reduced lateral force $\tilde f^* = \tilde\mu/\sqrt{1-\tilde\mu^2}$.

It is important to note that this threshold is *different* from the one that we obtained earlier by arguing that the tip becomes unstable at $x = \pi a/2$. Using the original quantities, the new threshold force reads

$$F_x^* = \frac{\mu a}{\sqrt{1-\mu^2 a^2}}(F_{\rm l}-F_z^*). \tag{18}$$

Moreover, it is interesting to note that due to lateral-normal coupling, the instability does not occur at a quarter of a lattice constant (which is $2\pi a$), but before, namely at

$$\cos(x^*/a) = a\mu, \tag{19}$$

which is obtained by substituting $\tilde f^* = \tilde\mu/\sqrt{1-\tilde\mu^2}$ into Eq. (17). It is therefore not possible to displace a particle laterally into another minimum without hysteresis effects. Subsequently, instability-induced energy loss cannot be avoided by applying a time-dependent lateral force without varying the normal load at the same time.

In Fig. 2, we show the dynamics of the island's center-of-mass for our default system (as defined by the values for the model's parameters that appear in the figure caption). Force amplitudes just below and just above the analytically calculated value for F^* are investigated. If F is just below F^*, the trajectory appears smooth in the analytical solution, despite the apparent cusp in $x_{\rm eq}(t)$. The numerical solution of the equations of motion is not included in the figure, as it would be right on top of the analytical solution. Once F exceeds F^*, there are moments in time where no analytical solution exists for quasi-static dynamics and we investigate the motion of the particle by solving the equations of motion numerically. One can see that the particle suddenly picks up momentum in x direction as it reaches the depinning point. Due to the normal lateral coupling, the island performs strong oscillations in its z coordinate. Note that the two trajectories resemble each other very closely as long as the particle driven with $F > F^*$ has not yet depinned.

It is also important to note that depinning may not be possible if the contact angle $\alpha_{\rm t}$ is too small, for instance when $\tan\alpha_{\rm t}$ exceeds the maximum slope that the island has to climb up the substrate's corrugation, see Fig. 1, In that case, the magnitude of the lateral force exerted by the substrate on the island grows more quickly with increasing F than the lateral component of the tip force. A phenomenon related to this argument may explain why it was not possible in the study reported in Ref. 1 to simply drag the islands in regular contact mode. This suggests that there is a critical angle $\alpha_{\rm t}^*$, below which depinning becomes impossible.

As one approaches $\alpha_{\rm t}^*$ from above by decreasing $\alpha_{\rm t}$, the critical force F^* will of course increase. Once $\alpha_{\rm t}$ becomes too small, the island cannot be pushed out of its original valley, which is a consequence of the cobblestone property of the model combined with the constant wedge-angle assumption. Criticality with respect to the impact angle $\alpha_{\rm t}$ is reached when F^* tends to infinity. At this point, we can neglect the load $F_{\rm l}$ as compared to F_z^* in Eq. (18)

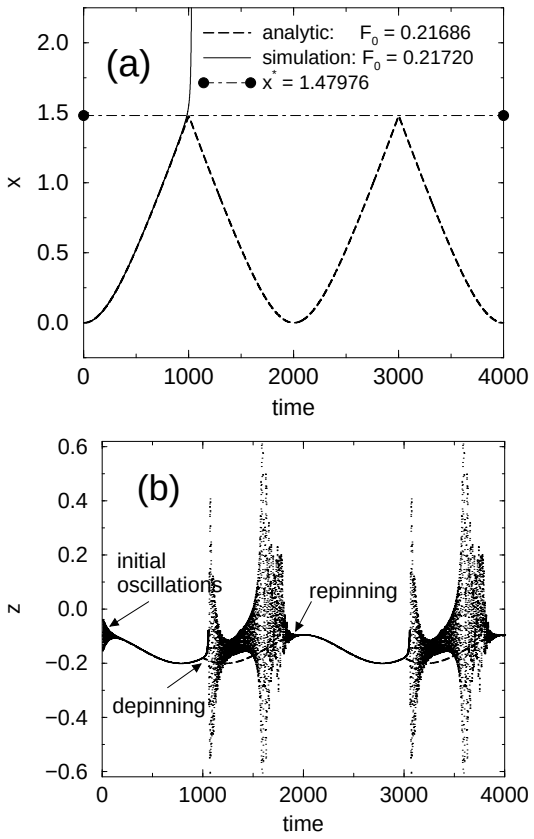

FIG. 2: Trajectory under a force $\mathbf{F} = F_0(1 - \cos(\omega_t)t)/2\ (\sin\alpha_t, -\cos\alpha_t)$ with $\omega_t = 2\pi/2000$ and $\alpha_t = 30^\circ$. (Note that the maximum amplitude of the force is F_0 and not $F_0/2$.) Two cases are considered, namely just below (dashed line from quasi-static solution) and above (solid line from simulation) threshold $F_0^* = 0.21694$ for a system with $a = 1$, $k_{xx} = 0.1k_{zz}$. (a) shows the trajectory in lateral and (b) shows the trajectory in normal direction. (The 'stiffnesses' k_{xx} and k_{zz} are introduced in Sec. III B and reflect a system described by $\mu = 0.0909...$). Damping is chosen to be $\gamma_x = \gamma_z = 0.04$. The dashed lines correspond to the analytic solution in Eq. (17), while the solid line (left) and the dots (right) represent respectively the x and the z coordinate of a particle as described in the simulation further below.

so that we obtain

$$\alpha_t^* = \mathrm{atan}\frac{\mu}{\sqrt{1-\mu^2 a^2}}. \tag{20}$$

This result will be confirmed in the result section along with an analysis what ratio of the energy will be dissipated due to normal motion.

B. Harmonic Approximation

With the full nonlinear potential V in Eq. (5), the full analytical solution of Eq. (7) is not attainable in closed form. However, sometimes, we are only interested in the oscillatory motion of the cluster around its equilibrium state or in the response of the system to a very small external force induced by the SFM tip. For such cases, we make a harmonic approximation. That is, we linearize the force induced by the full nonlinear potential in Eq. (5) around some equilibrium position $(x_{\mathrm{eq}}, z_{\mathrm{eq}})$ (which corresponds to using terms up to quadratic order in the Taylor expansion of the potential).

The general form of the equation of motion using this approximation reduces to one of a simple damped harmonic oscillator in two dimensions, namely

$$\begin{pmatrix}\ddot{x}\\ \ddot{z}\end{pmatrix} + \begin{pmatrix}\gamma_x & 0\\ 0 & \gamma_z\end{pmatrix}\begin{pmatrix}\dot{x}\\ \dot{z}\end{pmatrix} + \frac{1}{A}\begin{pmatrix}k_{xx} & k_{xz}\\ k_{zx} & k_{zz}\end{pmatrix}\begin{pmatrix}x - x_{\mathrm{eq}}\\ z - z_{\mathrm{eq}}\end{pmatrix} = \frac{1}{A}\begin{pmatrix}F_x\\ F_z\end{pmatrix}. \tag{21}$$

The coefficients k_{xx}, k_{xz}, k_{zx}, and k_{zz} of the quadratic terms in the harmonic potential are interfacial stiffness coefficients defined by

$$k_{xx} := \frac{\partial^2 V}{\partial x^2}\Big|_{(x_{\mathrm{eq}},z_{\mathrm{eq}})}, \quad k_{xz} := \frac{\partial^2 V}{\partial z \partial x}\Big|_{(x_{\mathrm{eq}},z_{\mathrm{eq}})}, \tag{22}$$
$$k_{zx} := \frac{\partial^2 V}{\partial x \partial z}\Big|_{(x_{\mathrm{eq}},z_{\mathrm{eq}})}, \quad k_{zz} := \frac{\partial^2 V}{\partial z^2}\Big|_{(x_{\mathrm{eq}},z_{\mathrm{eq}})}.$$

Assuming the lateral equilibrium coordinate x_{eq} has inversion symmetry (e.g., at $x_{\mathrm{eq}} = 0$), the mixed terms k_{xz} and k_{zx} of the stiffness matrix vanish in Eq. (21). Thus, in this section, we assume $x_{\mathrm{eq}} = 0$ and hence $k_{xz} = k_{zx} = 0$. We provide in Section III A an equilibrium analysis to derive expressions for the equilibrium coordinates $(x_{\mathrm{eq}}, z_{\mathrm{eq}})$ of the island; combined with the definitions in Eq. (22), that analysis explicitly gives the interfacial stiffness parameters in terms of the physical parameters in V and F.

Our primary motivation for studying the approximate model Eq. (21) is to derive estimates of the power loss P due to damping for a given applied force $\mathbf{F}$ in Eq. (8). Depending on the choice of $\mathbf{F}$ in Eq. (8), it is possible to find the analytic solution $x(t)$ for the equation of motion, Eq. (21), in closed form. Thus, it is possible to compute the maximum lateral deflection $x_{\max}$ for a given amplitude F_0 of the applied force. If F_0 is sufficiently large that $x_{\max} > \pi a$, the island has moved across a lateral peak in V, the full nonlinear potential in Eq. (5). In that case, the harmonic approximation does not really apply since the applied force would have pushed the island toward the next laterally adjacent minimum of V. Since the actual restoring force $\partial V/\partial x$ is maximized when $x = \pi a/2$ in Eq. (7), we shall look instead for a critical force amplitude F^* in Eq. (8) such that

$$x_{\max}^* = \frac{\pi a}{2} = \text{one quarter of a lattice constant.} \tag{23}$$

The critical force amplitude F^* at which Eq. (23) is satisfied in the harmonic approximation can be used to give an estimate on the threshold power P^* to displace the island from its stable position as mentioned in Section I.

Within standard linear-response theory, one can calculate the average power $\langle P\rangle$ dissipated into the damping terms

$$\langle P\rangle = A(\gamma_x\langle\dot{x}^2\rangle + \gamma_z\langle\dot{z}^2\rangle), \tag{24}$$

i.e., the contribution to $\langle P\rangle$ due to the motion parallel to x is given by

$$\langle P_x\rangle = \gamma_x A \sum_n \frac{n^2\omega_{\rm t}^2 \mid \tilde{F}_{x,n}/A \mid^2}{(k_{xx}/A - hn\omega_{\rm t})^2 + \gamma_x^2 n^2\omega_{\rm t}^2}. \tag{25}$$

Here we have used the relation between the Fourier coefficients $\tilde{x}_n$ and $\tilde{F}_{x,n}$, which follows from the first line in Eq. (21) and is given by

$$\left(-hn^2\omega_{\rm t}^2 + i\gamma_x n\omega_{\rm t} + k_{xx}/A\right)\tilde{x}_n = \frac{1}{A}\tilde{F}_{x,n} \tag{26}$$

A similar derivation applies for the contribution $P_z(t)$ related to the motion normal to the interface.

IV. RESULTS FOR THE THRESHOLD POWER

A. Low-frequency limit

In this section, we will consider driving under small frequencies, similar to the way in which the island is driven in Fig. 2. Indeed, the parameters listed in the caption of that figure are the default parameters used here.

It is easiest to discuss the motion at small values of the maximum driving force F_0, since then the harmonic approximation is valid. In that case, the island is well in the pinned regime. As $\omega_{\rm t}$ is small compared to all other frequencies in the system, we may approximate the (average) dissipated power given in Eq. (25) with

$$P_x \approx \frac{\gamma_x A}{2}\,\omega_{\rm t}^2\,\mathcal{A}_x^2, \tag{27}$$

where $\mathcal{A}_x = F_{0,x}/k_{xx}$ is the lateral amplitude of the oscillation. If one assumes that the harmonic approximation provides good estimates for the dissipated power even close to depinning, then one may estimate the dissipated threshold power (only the contribution that goes into the lateral damping) with

$$P_x^* \approx \frac{\gamma_x A}{2}\,\omega_{\rm t}^2\,\mathcal{A}_x^{*\,2}, \tag{28}$$

where $\mathcal{A}_x^*$ is the lateral amplitude at which the island depins, i.e., at $\mathcal{A}_x^* \approx 1.5$ in Fig. 2. Note that this value of $\mathcal{A}_x^*$ is close to a quarter of a lattice constant, which is where a 'naive' treatment would have expected depinning to occur.

A similar relation for the threshold power can be derived for the threshold power P_z^* due to the damping associated with the normal motion. However that approximation is less satisfying due to the non-monotonic behavior in the z component between the initial position and the depinning position. The non-monotonic form or the little peak in the z component, which can be seen on the right-hand side of Fig. 2 before depinning, reflects some 'extra motion'. This results in extra energy dissipation as compared to a case where the peak was not present.

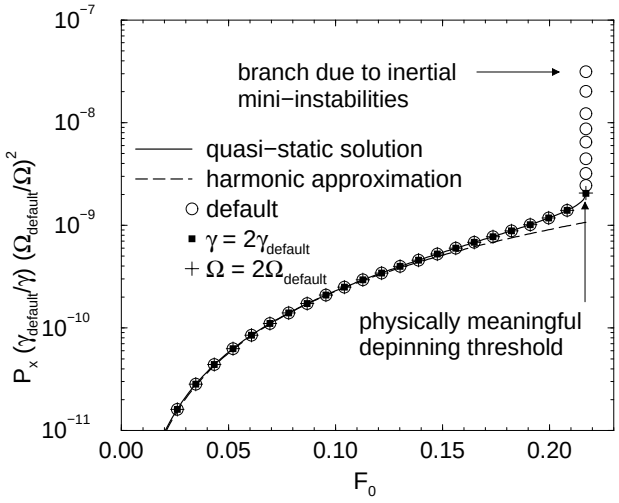

FIG. 3: Scaled dissipated power for different driving amplitudes in the low-frequency regime. Symbols are from simulations, while lines correspond to analytical theories according to Eq. (29), which contains the maximum force F_0 implicitly, see also Fig. 2. The end-point of the quasi-static solution is marked by an arrow. Due to inertial effects, the particle can be pushed with forces slightly above the analytical end-point force and nevertheless remain pinned. In that case, however, the particle departs from the quasi-static solution leading to increased dissipation. This branch is unstable against small fluctuations and therefore the end point of the analytical solution provides the physically relevant force and power threshold.

A rather reasonable approximation can be obtained by considering the quasi-static solution stated implicitly in Eq. (17). At every instance of time, we may approximate the velocity of the island by the vector $(\dot{x}_{\rm eq}, \dot{z}_{\rm eq})$. The power dissipated into the 'lateral' thermostat is then given by

$$P_x = \gamma_x A \left\langle \dot{x}_{\rm eq}^2 \right\rangle, \tag{29}$$

where $\langle\bullet\rangle$ denotes the average over one oscillation. In fact, if the time-scale separation is obeyed as well as for our default system, Eq. (29) is essentially exact. This is demonstrated in Fig. 3, where a full simulation (numerical integration of the 'true' equations of motion) is compared to the power obtained from Eq. (29). The simple harmonic approximation turns out surprisingly close to the exact solution. P_x^* is off by a factor of two close to depinning. This factor is not universal, but it depends on the impact angle $\alpha_{\rm t}$ and the coefficient $a\mu$.

In Fig. 3 we also included data, in which the driving

frequency ω_t and the phononic damping γ_x was changed by a factor of two. It can be seen that all curves superimpose rather nicely, if the dissipated power is rescaled to $P/\gamma\omega_t^2$, see Eq. (27). A feature that cannot be incorporated into the quasi-static solution is the occurrence of a new branch at an external driving force just a little above the theoretically predicted depinning force. The dissipated power seems to have an almost infinite slope with respect to F_0 near the predicted critical value F_0^*. The reason for this additional branch can be understood as follows: If F exceeds F_0^* just by a tiny amount, the system should become unstable. However, the time during which the depinning condition is satisfied is too short for the particle to react and the island moves only a very small distance into the 'depinned' area. In the meantime, the external lateral force has been reduced and the depinning condition is no longer satisfied. The particle then quickly moves back towards the proper $x_{\rm eq}$, similar to what was called a second-order instability in Ref. 15. It is obvious that an almost arbitrarily small thermal fluctuation would help an island to depin once it entered the depinned area. Therefore, this additional branch will be suppressed and the physically meaningful depinning occurs near the end point of the quasi-static solution.

In the low-frequency limit, the energy loss is obviously related to the phononic damping rather than to the static friction force or intrinsic energy barriers. It may nevertheless be difficult to exploit the equations derived in this section to determine a meaningful 'intrinsic' damping coefficient from measuring the power loss. One of the reasons is that we treated the damping coefficient as constant, which is certainly not true if the normal load fluctuates significantly during one oscillation. The harder we press the island into the substrate, the larger the viscous damping between the phonon baths[16]. This can be rationalized as follows: When the (surface) atoms fluctuate around their current equilibrium positions, the momentum transfer between two atoms from opposing surfaces will increase when they are more strongly pressed against each other. This will result in higher damping and does not require instabilities. The load-induced increase in damping may turn out small if the additional external normal force is small as compared to the adhesive load.

The other possible difficulty in relating measured powers to the damping coefficient is that one has to include the loss due to motion in the coordinate z, i.e., if the impact angle approaches zero, most of the energy will be dissipated into the normal direction. Our calculations, however, indicate that this effect becomes only relevant close to the critical impact angle α_t^*, below which the island cannot be depinned by means of a low-frequency excitation, see Fig. 4. In most of the cases, the power dissipated in normal direction is small as compared to that in lateral direction. This behavior can be expected to be rather generic, as the normal contact stiffness is typically much higher than the lateral contact stiffness. Therefore, the fluctuations normal direction to the interface will in most cases be small as compared to the lateral fluctuations.

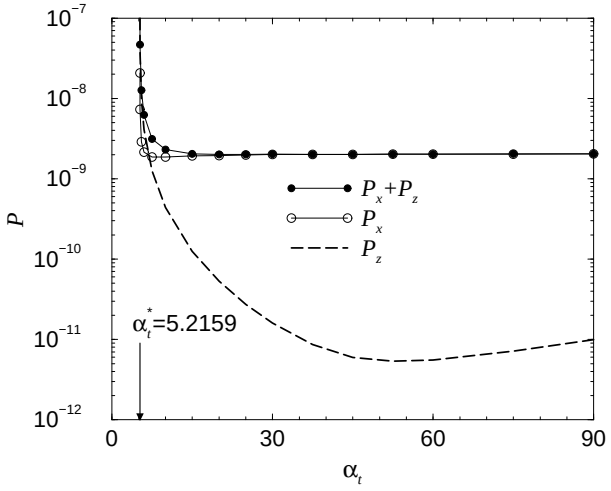

FIG. 4: Dissipated threshold power P^* as a function of the impact angle α_t. The two contributions P_x^* and P_z^* are shown as well. Except for α_t, all parameters are set to their default values. At and below α_t^*, the impact angle is too small to initiate sliding due to transverse normal coupling. The critical angle α_t^*, which follows from Eq. (20), is indicated by an arrow.

B. High-frequency limit

It may also be conceivable to assume that momentum is transferred from the tip to the sample quasi-instantaneously once per oscillation. Thus, unlike in the previous section, the system is not driven adiabatically. Since the tip frequency is the smallest frequency in the system, the situation can conveniently be described as an initial value problem. At time $t = 0^-$, the island is sitting in the point of minimum energy. It is then impacted at time $t = 0$ by the tip and receives an initial kinetic energy $\Delta E_{\rm initial}$. Since the particle is pushed in x direction and z direction, the initial velocity will have the lateral component $v_x(t = 0^+) = \sqrt{2\Delta E_{\rm initial}/m}\sin\alpha_t$ and the normal component $v_z(t = 0^+) = -\sqrt{2\Delta E_{\rm initial}/m}\cos\alpha_t$. Depending on the magnitude of $\Delta E_{\rm initial}$ the particle may have enough energy to escape its present location and move on to another minimum or remain stuck at its present location. Since the tip frequency is the smallest one in the system, it may be reasonable to assume that the island comes to rest before it is impacted again.

Within the harmonic approximation, lateral and normal motion decouple. Therefore, we may expect that the system depins if the energy in the lateral motion is sufficiently large to carry the island over the minimum energy barrier $\Delta E_{\rm min}$ given in Eq. (14). Using this simple picture, we would expect the separation between pinned and

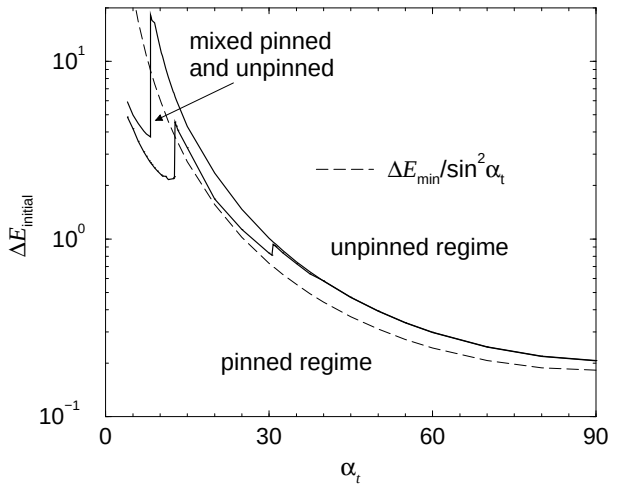

FIG. 5: The figure shows the regimes in which an initial amount of (kinetic) energy $\Delta E_{\rm initial}$ is sufficient or not sufficient to move an adsorbed particle from its ideal position towards the next minimum. The full lines were obtained from simulations. Between the two full lines, the pinned regime and the unpinned regime coexist. The dashed line is based on a simple estimate of the separation line between both regimes.

unpinned at a value $\Delta E^*_{\rm initial}$

$$\Delta E^*_{\rm initial} = \frac{\Delta E_{\rm min}}{\sin^2\alpha_{\rm t}}. \qquad (30)$$

While this equation would be essentially exact in the one-dimensional case, it can only provide a rough guideline in higher dimensions for mainly three reasons: (a) Particles constantly lose energy into the damping term while moving on the surface. Thus some (small) amount of energy is lost before the first escape attempt. (b) The particles will not move on the adiabatic or 'optimum path' and hence they will most likely not cross the barrier at its optimum point. (c) Because lateral and normal motion couple, kinetic energy can be transfered from normal to lateral motion. This can help the particle escape from its minimum. If $\alpha_{\rm t} = 90°$, $\Delta E^*_{\rm initial}$ will be underestimated due to reasons (a) and (b). However, at sufficiently small values of $\alpha_{\rm t}$, one may also overestimate $\Delta E^*_{\rm initial}$ due (c). It nevertheless turns out that Eq. (30) provides a reasonable estimate for $\Delta E^*_{\rm initial}$ in our default system, provided that $\tan\alpha_{\rm t}$ is not smaller or in the vicinity of the (differential) friction coefficient $\partial F_{\rm s}/\partial F_{\rm l}$. This can be seen in Fig. 5, where the pinned and unpinned regimes are shown as a function of $\alpha_{\rm t}$ and $\Delta E_{\rm initial}$.

In Fig. 5, one can also learn that there is not a unique separation line between 'pinned' and 'unpinned'. The upper and the lower curve simply state an upper bound for $\Delta E_{\rm initial}$ in the pinned phase and a lower bound for $\Delta E_{\rm initial}$ in the unpinned phase. In between the two curves, there are both 'pinned' and 'unpinned' regions. Thus due to the lateral-normal coupling, an increase in initial kinetic energy might not necessarily unpin the islands in these regions.

The origin of the discontinuities in Fig. 5 is related to the lateral normal coupling. Since the motion is not one dimensional, there is no unique way to cross the barrier. In particular, it can help the particle to rock back and forth a few times before crossing the barrier when hit under a small angle. This may shuffle kinetic energy from the normal motion into lateral motion. Whenever a new barrier-crossing mode sets in upon lowering the impact angle, it has become beneficial for the particle to rock back and forth $n+1$ times instead of n times before crossing.

V. CONCLUSIONS

We studied the motion of an essentially rigid cluster (nanoparticle) that is pushed over a substrate surface under the influence of a tip impacting at an angle $\alpha_{\rm t}$. While the actual behavior of the particle will be more complex than our model, which does not implicitly include elastic deformation of particle and substrate, we believe that some generic ingredients are contained in our model. Most importantly, the effect of the coupling of normal and transverse motion is incorporated. Two limiting regimes were identified in our model: An adiabatic regime ("low-frequency limit") and a momentum-transfer regime ("high-frequency limit"). The mechanism for power loss is different in the two regimes.

In the adiabatic regime, the viscous-type damping forces determine the dissipated power. The impact angle $\alpha_{\rm t}$ is rather irrelevant unless the critical angle $\alpha^*_{\rm t}$ is approached below which the particle cannot be moved even under an arbitrarily large external force amplitude. The reason for the irrelevance of $\alpha_{\rm t}$ in the adiabatic regime is that the amplitude in transverse motion can almost always be expected to significantly exceed that of the normal motion. Since normal and transverse damping should be in the same order of magnitude, the loss is mainly due to transverse motion. A critical angle $\alpha^*_{\rm t}$ exists because increasing the external force does not only push the island harder to the side but also deeper into the substrate. This in turn increases the lateral force that the substrate exerts on the adsorbed nanoparticle and prevents sliding at $\alpha_{\rm t} < \alpha^*_{\rm t}$.

In the momentum-transfer regime, the observed energy loss mainly depends on the energy barriers in the system rather than on the damping forces. This can be understood in the following simplistic picture, which turns out to provide a reasonable guideline provided the cantilever period is the smallest characteristic time scale in the system: The adsorbed particle is given an initial (kinetic) energy each time it is hit. This energy is completely dissipated before the particle is impacted again. The initially provided kinetic energy can be decomposed into a longitudinal or into a transverse component. If the "longitudinal energy" exceeds the intrinsic barrier for sliding,

then the system can (and will) depin.

We will now turn to the discussion of experiments with an emphasis on Ritter et al.'s study.[1] When adsorbed nanoparticles or islands are manipulated nondestructively in contact mode,[2–4] then one will certainly be in the low-frequency limit. However, in this case, the friction forces can be measured directly anyway. Similarly, we would presume this mode to apply to in the experiments by Wang et al.[5] and Miura et al.,[7] where the islands moved are essentially acting as spacers between tip and substrate, mediating the pressure exerted by the SFM tip.

Conversely, when nanoparticles are moved in tapping mode,[1,6] it seems as if the energy barriers are the relevant factor for the dissipated power, at least as far as the islands with a size larger than 10,000 nm^2 are concerned. While it would be desirable to support such a statement from simulations, given the simplicity of the present treatment, the most convincing argument for this assumption must come from the experiment itself. No matter which model we assume for the interpretation of the experimental data, the frictional stresses will turn out to be roughly in the order of 10^8 Pa as can be deduced from Fig. 4 in Ref. 1. This value is many orders of magnitudes larger than what one would expect from any Stokes type damping mechanism given the moderate experimental maximum velocities $v_{\max}$ of the islands. (This statement is easily supported by estimating the slip time $\tau_{\rm slip}$, which – being the inverse of γ – is a measure for damping.[8] Equating the dissipated power P with $mv^2/\tau_{\rm slip}$ and using the available experimental data yields a value of $\tau_{\rm slip} \approx 10^{-17}s$, which is about 5 orders of magnitudes smaller than the smallest period of a phonon in the materials involved and thus unphysical.) Hence one can rule out the low-frequency limit to be applicable. Of course, as discussed in Ref. 1, only sufficiently large islands that are internally strained show measurable threshold power, while small, homogeneous, disordered particles are displaced extremely easily. As Ritter et al. find a rather well-defined value for the threshold power of an individual island (at least for the second, third, and consecutive depinning events) and since the islands move easily once this power is exceeded, the data is consistent with a picture in which the nanoparticles explore the energy barriers that need to be overcome to invoke sliding.

An interesting aspect of the experiments by Ritter et al. is that due to their new approach, the experiments open possible avenues to investigate the frictional properties of a nanoscale contact between atomistically flat surfaces. If A is the contact area of the flat interface between unlubricated three-dimensional solids, assuming that at least one of the two surfaces is disordered and that no plastic deformation occurs, theoretical arguments in Ref. 11 suggest that the friction force should be proportional to $\sqrt{A}$ (interfaces between perfect crystals behave differently[17]). Assuming the antimony island is disordered in each trial, by sampling various island sizes, it would in principle be possible to verify this claim. Such experiments could provide a more direct test of the $\sqrt{A}$ hypothesis than earlier SFM experiments that typically used curved tips and hence involved more complicated contact mechanics (see, e.g., 18–22). However, the Ritter results, which cover island sizes between 10,000 nm^2 and 110,000 nm^2, feature a linear dependence of the dissipated power on the contact area. As an explanation, the authors speculate that the nanoparticles manipulated within their study are already too big to move as essentially rigid bodies, and dissipation by elastic multistabilities might consequently be the cause for the observed relatively high dissipation. Moreover, the particles above 10,000 nm^2 are internally strained while the particles below 10,000 nm^2 appear unstrained, which supports this interpretation. Nevertheless, their study indicates that small islands below 10,000 nm^2 might be small enough to move as rigid bodies. Such islands, however, were not explicitly included in their present study.

Acknowledgments

MHM acknowledges support from the National Sciences and Engineering Research Council of Canada (NSERC) and Sharcnet.

* Correspondig author. Electronic address: mmuser@uwo.ca

[1] C. Ritter, M. Heyde, B. Stegemann, K. Rademann, and U. D. Schwarz, Phys. Rev. B, submitted.

[2] E. Meyer, R. Overney, D. Brodbeck, L. Howald, R. Lüthi, J. Frommer, and H.-J. Güntherodt, Phys. Rev. Lett. **69**, 1777 (1992).

[3] R. Lüthi, E. Meyer, H. Haefke, L. Howald, W. Gutmannsbauer, and H.-J. Güntherodt, Science **266**, 1979 (1994).

[4] P. E. Sheehan and C. M. Lieber, Science **272**, 1158 (1996).

[5] J. Wang, K. C. Rose, and C. M. Lieber, J. Phys. Chem. B **103**, 8405 (1999).

[6] M. Heyde, B. Cappella, H. Sturm, C. Ritter, and K. Rademann, Surf. Sci. **476**, 54 (2001).

[7] K. Miura, S. Kamiya, and N. Sasaki, Phys. Rev. Lett. **90**, art. no. 055509 (2003).

[8] M. H. Müser, M. Urbakh, and M. O. Robbins, Adv. Chem. Phys. **126**, 187 (2003).

[9] A. M. Homola, J. N. Israelachvili, M. L. Gee, and P. M. McGuiggan, Trans. ASME, J. Tribology **111**, 675 (1989).

[10] W. Steele, Surf. Sci. **36**, 317 (1973).

[11] M. H. Müser, L. Wenning, and M. O. Robbins, Phys. Rev. Lett. **86**, 1295 (2001).

[12] V. Zaloj, M. Urbakh, and J. Klafter, Phys. Rev. Lett. **82**, 4823 (1999).

[13] P. Berthoud and T. Baumberger, Proc. R. Soc. London A **454**, 1615 (1998).
[14] E. Gnecco, R. Bennewitz, T. Gyalog, and E. Meyer, J. Phys.: Condens. Matter **13**, R619 (2001).
[15] M. H. Müser, Phys. Rev. Lett. , **89**, art. no. 224301 (2002).
[16] Using elastic walls similar to those in Ref. 11 and cutting off adhesive interactions between the walls, we found that damping increases approximately linearly with the load.
[17] M. H. Müser, Europhys. Lett. **66**, 97 (2004).
[18] R. W. Carpick, N. Agrait, D. F. Ogletree, and M. Salmeron, J. Vac. Sci. Technol. B **14**, 1289 (1996).
[19] E. Meyer, R. Lüthi, L. Howald, M. Bammerlin, M. Guggisberg, and H.-J. Güntherodt, J. Vac. Sci. Technol. B **14**, 1285 (1996).
[20] M. A. Lantz, S. J. O'Shea, M. E. Welland, and K. L. Johnson, Phys. Rev. B **55**, 10776 (1997).
[21] U. D. Schwarz, O. Zwörner, P. Köster, and R. Wiesendanger, Phys. Rev. B **56** 6987 (1997).
[22] L. Wenning and M. H. Müser, Europhys. Lett. **54**, 693 (2001).